The final publication is available at Springer via http://dx.doi.org/10.1515/chempap-2016-0058

Synthesis, structural and spectroscopic properties of asymmetric Schiff bases derived from 2,3-diaminopyridine

[a]Agnieszka Pazik , [a]Beata Kamińska, [a]Anna Skwierawska, [b]Łukasz Ponikiewski

[a]*Department of Chemistry and Technology of Functional Materials,* [b]*Department of Inorganic Chemistry, Gdansk University of Technology, Narutowicza Street 11/12, 80-233 Gdansk, Poland*

Two Schiff base derivatives, 4-(2-amino-3-pyridyliminomethyl)phenol (*I*) and 3-(2-amino-3-pyridyliminomethyl)nitrobenzene (*II*), were synthesised and characterised by spectroscopy. The structure of *I* was determined by single crystal X-ray diffraction studies. The asymmetric Schiff base derived from 2,3-diaminopyridine selectively recognise transition and heavy metal cations, and some anion. Ligands *I* and *II* form stable complexes with Cu^{2+}, Zn^{2+}, Pb^{2+}, Al^{3+} whereas ligand *I* also binds F^- ions. The stoichiometry for the host : cation is 1 : 1 and 2 : 1. The addition of F^- ion in CH_3CN to ligand *I* causes a colour change of the solution from colourless to yellow. The binding behaviour of ligand *I* towards several ions was investigated using density functional theory calculations.

Keywords: asymmetric Schiff bases, X-ray crystal structure, cation complexation, fluoride, UV-VIS spectroscopy, ^{1}H NMR spectroscopy

Introduction

Schiff bases have received a great deal of attention in a wide variety of fields due to their simple synthesis and various applications. They can be readily synthesised by simple one-pot condensation of aldehydes and primary amines in an alcoholic solvent under anhydrous conditions (Schiff, 1866). Schiff bases have played an important role in the development of coordination chemistry, as they can form stable complexes with most of the transition metals. One of the oldest-known classes of Schiff base ligands used in organic synthesis is the salen derivatives (Kleij et al., 2005; Şahin et al., 2010).

Schiff bases and their metal complexes are catalysts for many reactions (e.g. oxidation (Ourari et al., 2012), epoxidation (Grivani & Akherati, 2013), reduction (Ji et al., 2008), polymerisation (Zhang et al., 2008), ring-opening polymerisation (Yao et al., 2012) and Diels–Alder (Jarvo et al., 2005), Henry (Zhou et al., 2012a) and Mizoroki–Heck reactions (Heo et al., 2012)). Their antibacterial (Amin et al., 2012; Dai & Mao, 2013), antifungal (Abdel-Rahman et al., 2013; Carreńo et al., 2015), antiviral (Kumar et al., 2010) and anti-tumour (Qiao et al., 2011) activities have been revealed. Furthermore, heteroaromatic Schiff bases as complexones have often been applied to the analytical determination of heavy metal ions in the environmental samples (Afkhami et al., 2012) as well as ionophores for ion-selective electrodes (Jeong et al., 2005; Yuan et al., 2012).

The recognition and sensing of ions by appropriately designed ion receptors is the primary objective of a number of groups of chemists. Due to the wide variety of cations that are important for living organisms. A number of detection methods are time-consuming and require high-quality analytical instrumentation, hence it is important to design and synthesise sensing materials for transition metal ions and heavy metal ions. Sensors that change colour upon host-guest interactions are of use in simple naked-eye applications without requiring any expensive equipment. Moreover,

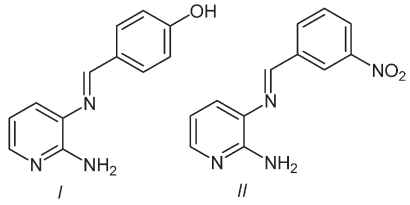

Fig. 1. Chemical structure of ligands *I* and *II*.

in recent research a number of Schiff bases have been used as highly selective fluorescent chemosensors (Devaraj et al., 2012; Azadbakht et al., 2013; Aziz, 2013; Jiménez-Sánchez et al., 2013) and colorimetric sensors for cations (Gupta et al., 2013; Yang et al., 2013). However, only a few reports describe ligands with appropriate applications in aqueous media (Udhayakumari et al., 2012; Zhou et al., 2012b).

It is also worth noting the important role played by anions; because of their significant impact on human lives, and chemical and biological processes, the easy detection of such species by readily accessible (synthetic) receptors is desired. To date, cationic receptors are widely known, while anion receptors remain obscure. To the best of our knowledge, only a few Schiff bases serving as anion receptors have been synthesised to date (Erdemir et al., 2013; Huang et al., 2013; Kumar et al., 2013; Lin et al., 2013; Liu & Shao, 2013; Reena et al., 2013; Sen et al., 2013).

The present study was focused on the synthesis of ligands for the selective recognition of either transition metal or heavy metal cations, and the detection of anions. Ligands *I*, *II* with different positions of the substituent attached to the molecule relative to the CN double bond were investigated and their selectivity towards ions was compared (Fig. 1). To the best of our knowledge, the ion recognition ability of *I* and *II* has not been examined using UV-VIS or ^{1}H NMR spectroscopy and has not yet received attention in the literature. Furthermore, according to recent research, some Cu(II), Zn(II) and Ni(II) complexes with Schiff base *I* exhibit antibacterial activities (Jeewoth et al., 1999). UV-VIS spectroscopic studies show that both compounds (*I* and *II*) are able to form complexes with Cu^{2+}, Zn^{2+}, Pb^{2+} and Al^{3+} ions. In addition, compound *I* is a potential sensing F^- receptor. Ligand *I* with strong hydrogen bonds and the *para*-substituted hydroxyl group, upon the addition/influence of an anion guest changes colour in association with changes in the electronic properties of chromogenic units. The present study also includes a theoretical investigation of the nature of the binding behaviour of compounds using the DFT method.

Experimental

Schiff base ligands *I* and *II* were synthesised following the procedure presented in Fig. 2. 2,3-

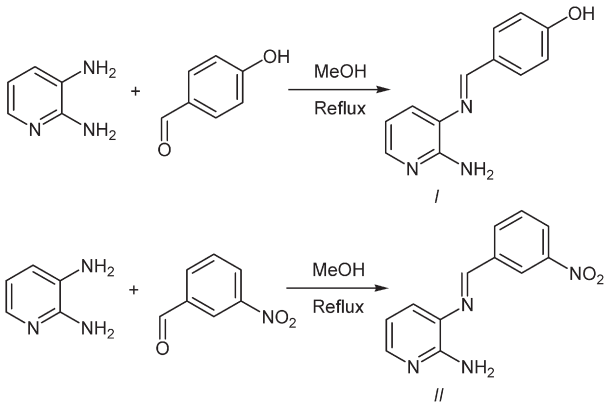

Fig. 2. Synthesis of Schiff bases *I*–*II*.

Diaminopyridine, 4-hydroxybenzaldehyde and 3-nitrobenzaldehyde were obtained from Sigma–Aldrich (Poland). The metal salts used for UV-VIS spectrophotometric titrations (perchlorates: $Zn(ClO_4)_2 \cdot 6H_2O$, $Cu(ClO_4)_2 \cdot 6H_2O$, $Co(ClO_4)_2 \cdot 6H_2O$, $Ni(ClO_4)_2 \cdot 6H_2O$, $Cd(ClO_4)_2 \cdot 6H_2O$, $Pb(ClO_4)_2 \cdot 3H_2O$) and $Al(NO_3)_3 \cdot 6H_2O$ were of analytical grade and were purchased from Sigma–Aldrich. All anions, in the form of tetrabutylammonium salts (from Sigma–Aldrich), were stored in desiccators under vacuum. Acetonitrile was dried over calcium hydride prior to use. Other solvents employed in the synthesis and experiments were of extra-pure grade and used as received without further purification.

^{1}H NMR spectra were recorded for the samples dissolved in DMSO-d_6 at 500 MHz on a Varian instrument. The chemical shifts (δ) are given in parts per million (ppm) relative to TMS and the coupling constants (J) are reported in hertz (Hz). Elemental analyses were performed on an EAGER 200 apparatus. The FT-IR spectra for samples in dry KBr were taken on a Genesis II FT-IR (Mattson) instrument. Gaussian 03 software was used for all theoretical calculations (Frisch, 2003). The ground-state optimisation was carried out using Gaussian 03 software with B3LYP and 6-31++G(dp) basis set at the density functional theory (DFT) level. Thin layer chromatography (TLC) analyses were performed on aluminium plates coated with silica gel 60 F254 (Merck). UV-VIS measurements were carried out at ambient temperature with the use of a UNICAM UV 300 series spectrophotometer. UV-VIS titrations were carried out in a 1 cm path length quartz cuvette maintaining a constant volume for the *I* and *II* solutions (2 mL).

General experimental procedure for synthesis of ligands I–II

The synthesis procedure was adapted from the literature (Dubey & Ratnam, 1977; Cimerman et al., 1997). To a heated solution of 2,3-diaminopyridine

(5 mmol, 0.546 g) dissolved in dry MeOH (10 mL) a solution of the appropriate aldehyde (5 mmol in 10 mL of MeOH) was slowly added drop-wise. The mixture was stirred overnight at 50 ℃. After that time, the solvent was removed under reduced pressure and the resulting crude product was recrystallised from 2-propanol. Compound *I* was purified by gradient column chromatography on silica gel, using a $CHCl_3$–MeOH solvent mixture.

X-ray structure analysis of ligand I

4-(2-Amino-3-pyridyliminomethyl)phenol (*I*) single crystal was grown from a $CHCl_3$–MeOH mixture by a slow solvent evaporation. For the X-ray studies, a transparent crystal of needle shape was selected. The experimental data were collected on a KUMA KM4 diffractometer with graphite monochromated MoK_α radiation using a Sapphire-2 CCD detector. The apparatus was equipped with an open flow thermostat (Oxford Cryosystems, UK) which made it possible for the experiments to be carried out at 298 K. Data reduction, space group determination, solution and refinement were effected using the CrysAlisPro software package (Version 1.171, 2008, Oxford Diffraction, Abingdon, UK). The structure was resolved by the direct method and refined by full-matrix least-squares on F^2 (all data) using the shelxl program package (Sheldrick, 2008). The basic crystal data, descriptions of the diffraction experiment and details of the structure refinement are given in Table 1.

All non-hydrogen atoms were refined anisotropically. The N—H, O—H hydrogen atoms and H6A, H18A were located in a difference Fourier map and refined freely; N2—H2B 0.92(3) Å, N2—H2C 0.84(3) Å, N5—H5B 0.93(3) Å, N5—H5C 0.88(3) Å, O1—H1A 1.00(3) Å, O2—H2A 0.95(3) Å, C6—H6A 1.03(2) Å, C18—H18A 1.02(2) Å. Other H atoms were positioned geometrically and refined using a riding model C—H = 0.93 Å, U_{iso}(H) = 1.2U_{eq}(C).

Table 1. Summary of crystal data, data collection and refinement for 4-(2-amino-3-pyridyliminomethyl)phenol

Parameter	Value
Empirical formula	$C_{24}H_{22}N_6O_2$
Formula mass/Da	426.48
T/K	298.15
Crystal system	Monoclinic
Space group	$P21/n$
Unit cell dimensions	
a/Å	9.8550(9)
b/Å	13.9442(7)
c/Å	16.2245(10)
β/°	104.975(7)
V/Å^3	2153.9(3)
Z	4
ρ/(g cm^{-3})	1.325
μ/(mm^{-1})	0.088
F(0 0 0)	896
Crystal size/mm^3	0.23 × 0.22 × 0.20
Index ranges	$-12 \leq h \leq 12$ $-15 \leq k \leq 17$ $-7 \leq l \leq 20$
Reflections collected	7954
Unique reflections	4224 (R_{int} = 0.0260)
Parameters	321
θ, range for data collections/°	2.58–28.49
S (goodness-of-fit)	1.053
R_1 [$I > 2\sigma(I)$]	R_1 = 0.0516; wR_2 = 0.1228
R indices (all data)	R_1 = 0.0814; wR_2 = 0.1456
Largest differences in peak and hole/(e Å^{-3})	0.244 and –0.160

Results and discussion

Synthesis and X-ray characterisation

The Schiff bases *I* and *II* were synthesised following the procedure detailed in the literature by heating 2,3-diaminopyridine and appropriate aldehyde in dry methanol (Fig. 2). Investigations into this group of compounds began as early as 2005. This problem was studied by Kleij et al. (2005), who synthesised the compounds under milder conditions and with higher yields of products (70 %). The reaction was carried out in methanol at ambient temperature for 24 h. The reaction can be adopted as a general method for synthesised compounds with an O—H group in the *ortho* positions relative to an imino group. The yield of the reaction appears to depend on the existence of a strong an intramolecular hydrogen bond.

The synthesised compounds were characterised on the basis of spectroscopic methods including FT-IR, UV-VIS, ^{1}H NMR and elemental analysis (Tables 2 and 3). For ligand *I*, the X-ray structure was also determined. The presence of free amino groups in the molecules was confirmed by the appearance of a singlet at δ around 5.83 and 6.13 in the ^{1}H NMR (DMSO-d_6) spectroscopy. The addition of D_2O caused the loss of signals corresponding to the 2-amino protons in pyridine.

The singlet at δ of 8.52 (*I*) and 8.85 (*II*) is ascribed to the CH═N proton (Waldeck, 1991; Schilf et al. 2004; Yıldız et al., 2009). The OH proton in ligand *I* appears at δ of 10.1. The chemical shifts, observed for *I* between the δ of 6.54–7.82 and for *II* 6.59–7.80 are ascribed to the aromatic protons. Comparing the ^{1}H NMR data of aromatic protons of compounds *I* and *II*, the different location of substituent attached to the molecule can clearly be seen.

The formations of Schiff base units in the FT-IR

Table 2. Data characterising prepared compound

Compound	Formula	M_r	w_i(calc.)/% w_i(found)/%			Yield	M.p.
			C	H	N	%	℃
I	$C_{12}H_{11}N_3O$	213.09	67.59	5.28	19.71	41	217–220
			67.52	5.31	19.68		
II	$C_{12}H_{10}N_4O_2$	242.08	59.50	4.16	23.13	45	198–200
			59.55	4.19	23.15		

Table 3. Spectral data of compounds

Compound	Spectral data
I	IR, $\tilde{\nu}$/cm^{-1}: 452, 496, 520, 598, 629, 644, 697, 773, 794, 836, 919, 953, 983, 1032, 1100, 1136, 1161, 1161, 1178, 1178, 1251, 1252, 1272, 1305, 1410, 1463, 1505, 1574, 1582, 1618, 2340, 2678, 3358, 3463 ^{1}H NMR (500 MHz, DMSO-d_6), δ: 5.83 (s, 2H, NH_2), 6.54 (dd, J_1 = 4.88 Hz, J_2 = 7.33 Hz, 1H), 6.86 (d, J = 8.3 Hz, 2H), 7.31 (d, J = 7.33 Hz, 1H), 7.79 (d, J = 4.89 Hz, 1H), 7.82 (d, J = 8.79 Hz, 2H), 8.52 (s, 1H), 10.1 (s, 1H, OH) ^{1}H NMR (500 MHz, DMSO + D_2O), δ: 6.59 (dd, J_1 = 4.88 Hz, J_2 = 7.32 Hz, 1H), 6.85 (d, J = 8.3 Hz, 2H), 7.30 (d, J = 7.33 Hz, 1H), 7.72 (d, J = 4.88 Hz, 1H), 7.80 (d, J = 8.3 Hz, 2H), 8.46 (s, 1H)
II	IR, $\tilde{\nu}$/cm^{-1}: 428, 524, 564, 668, 693, 731, 768, 793, 850, 923, 968, 1099, 1180, 1255, 1311, 1347, 1433, 1467, 1518, 1605, 3127, 3241, 3471 ^{1}H NMR (500 MHz, DMSO-d_6), δ: 6.13 (s, 2H, NH_2), 6.58 (dd, J_1 = 4.88 Hz, J_2 = 7.33 Hz, 1H), 7.45 (d, J = 7.33 Hz, 1H), 7.78 (t, J = 8.30 Hz, 1H), 7.88 (d, J = 4.88 Hz, 1H), 8.33 (d, J = 7.81 Hz, 1H), 8.47 (d, J = 7.82 Hz, 1H), 8.79 (s, 1H), 8.85 (s, 1H) ^{1}H NMR (500 MHz, DMSO + D_2O), δ: 6.61 (dd, J_1 = 5.37 Hz, J_2 = 7.32 Hz, 1H), 7.35 (d, J = 6.35 Hz, 1H), 7.72 (t, J = 8.30 Hz, 1H), 7.80 (d, J = 3.42 Hz, 1H), 8.26 (d, J = 7.81 Hz, 1H), 8.34 (d, J = 7.81 Hz, 1H), 8.69 (s, 1H), 8.73 (s, 1H)

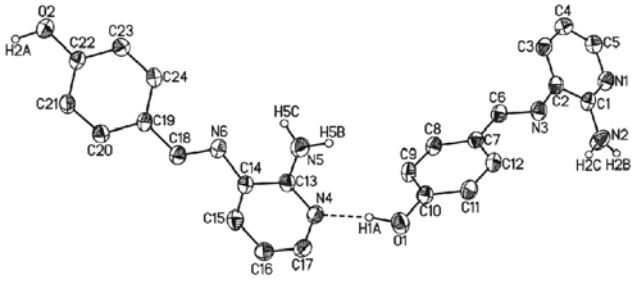

Fig. 3. ORTEP plot of *I*, showing atom-labelling scheme. Displacement ellipsoids are drawn at 50 % probability level.

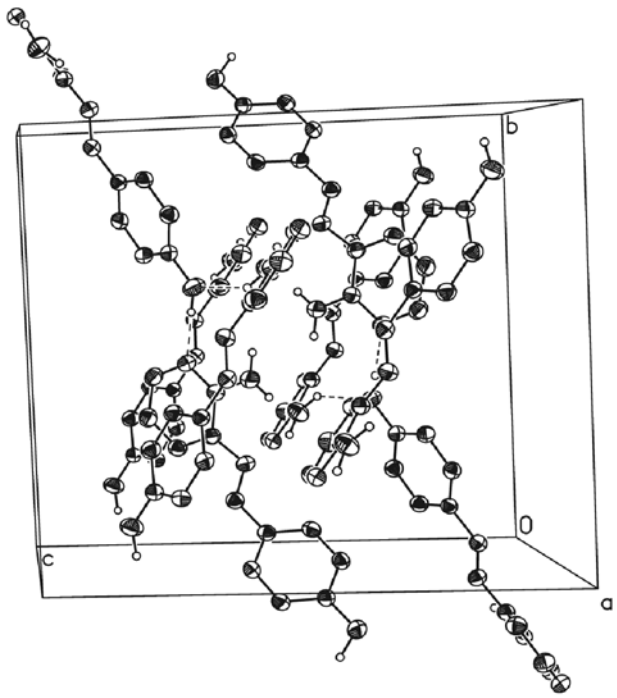

Fig. 4. X-ray crystal packing for ligand *I*.

spectrum can be observed in the absence of the bands between 1715–1645 cm^{-1} assignable to the characteristic C═O stretching vibration's. The CH═N groups stretching vibration appears between 1618–1605 cm^{-1} for both compounds. The FT-IR spectra of the ligands *I* and *II* show strong-intensity absorption bands at 3463–3471 cm^{-1} assigned to the N—H stretching mode. The spectrum of compound *I* also showed bands at about 2678 cm^{-1} and 2340 cm^{-1} which are assigned to the stretching hydrogen motions in the intramolecular O—H···N hydrogen bonding between the OH proton and the nitrogen atoms.

A drawing of the X-ray structure and crystal packing of *I* is shown in Figs. 3–5. X-ray analysis confirmed that the compound only existed in the phenolimine form. The asymmetric unit cell contains two

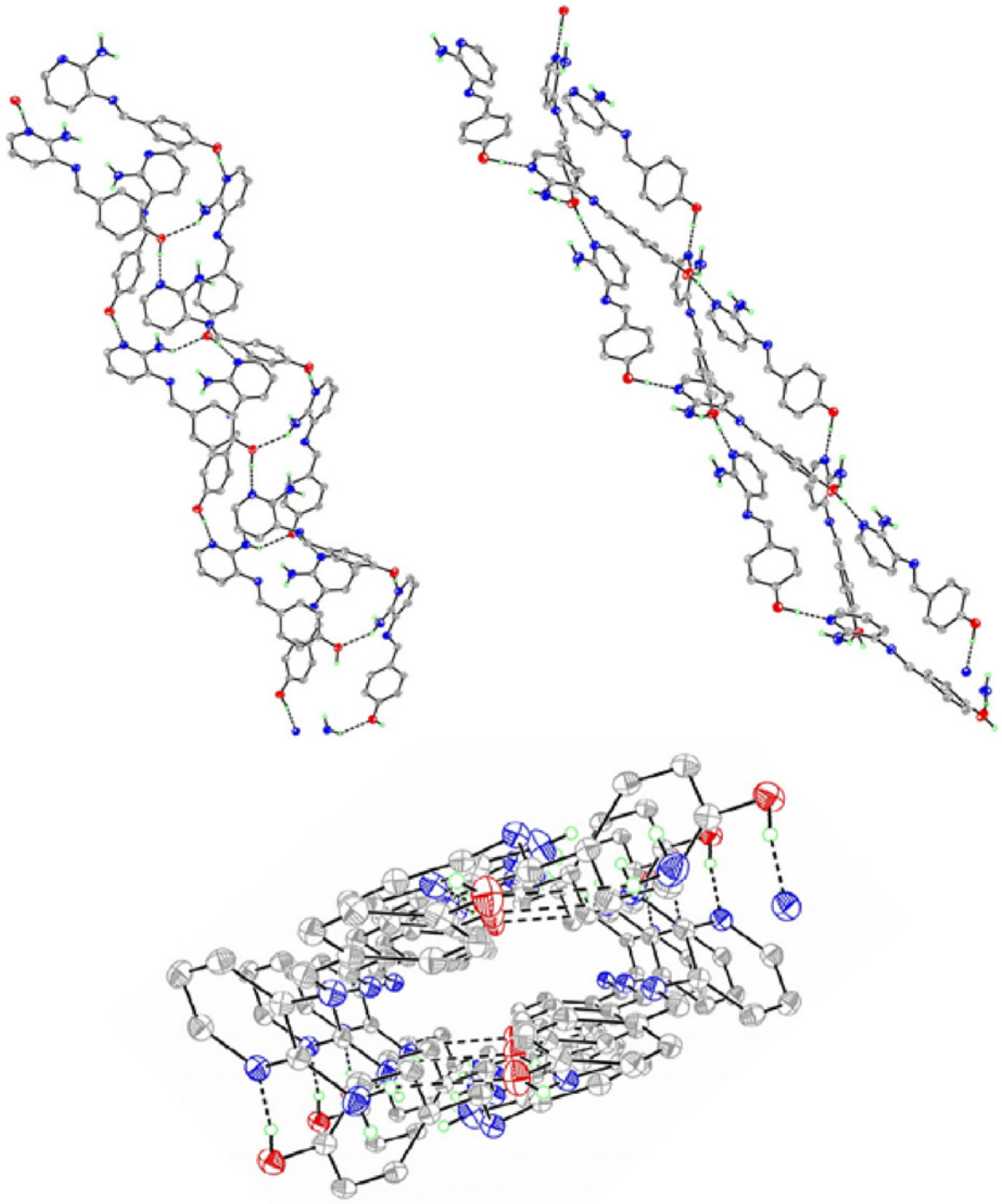

Fig. 5. Formation of left-handed and right-handed helix of ligand *I*.

unique molecules of compound *I* presented in Fig. 3. They are joined by the hydrogen bond formed between the hydroxyl group and the nitrogen of the pyridine ring of the second molecule of the compound. The hydroxyl group acts as the donor of the hydrogen bond to nitrogen atom of pyridine with O···N distances of 2.763(2) Å (O1···N4) and 2.723(2) Å (O2···N1) and O—H···N angles of 172(3)° (O1—H1A···N4), and 171(3)° (O2—H2A···N1) (Table 4). The hydrogen bonds form a one-dimensional single chain along the *b* axis. The amino group of the same pyridine ring acts as a donor of the next hydrogen bond to the oxygen of the hydroxyl group of the next molecule of the compound with N···O distances of 3.058(19) Å (N5···O2) and N5—H5C···O2 angles of 140(2)°. The presence of the hydrogen bond results in the formation of a left-handed helix built by three single chains. The compound so obtained crystallises

in the monoclinic system and belongs to the $P2_1/n$ space group. Hence, the unit cell contains both chains – left-handed and right-handed helix (Fig. 5).

In the case of a mono Schiff base derived from 2,3-diaminopyridine and salicylaldehyde, the strong intramolecular H-bonding is formed between O—H···N=C (Cimerman et al., 1992). The bond length O···N corresponding to a double bond is 2.649(4) Å which for compound *I* is not very probable. The X-ray powder diffractograms show similarities in the pyridine and benzene rings.

Spectroscopic studies

Nowadays, the design of a potential sensor for anions and cations such as transition metal ions, and heavy metal ions is very important from the medical perspective. High selectivity is a matter of necessity in an excellent sensor. The ion recognition properties of ligands *I–II* were investigated visually by colour change, ^{1}H NMR and UV-VIS spectroscopic methods.

The visual colour change in CH_3CN was investigated upon the addition of various ions. No colour and spectral changes were observed in the presence of alkali metal and alkaline earth metal cations. In the naked eye experiments, ligand *I* ($c = 3 \times 10^{-5}$ mol L^{-1}) showed a noticeable colour change from colourless to pale yellow in the presence of F^- ions (10 eq.) (Fig. 6). Ligand *II* did not exhibit any detectable colour change upon the addition of various ions. The presence of the —NO_2 substituent exhibiting an electron-withdrawing effect on the hydrogen properties did not provide colorimetric and spectral sensing ion recognition.

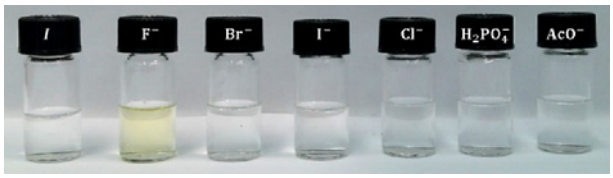

Fig. 6. Naked-eye colour change of ligand *I* ($c = 3 \times 10^{-5}$ mol L^{-1}) after addition of 10 eq. of various anions ($c = 10^{-4}$ mol L^{-1}) in CH_3CN solvent.

In the preliminary experiments, the anion binding properties of ligands in the UV-VIS spectrum in CH_3CN were investigated. The most significant changes for ligand *I* in the absorption spectra were observed in the presence of tetra−1-butylammonium fluoride. UV-VIS titrations were carried out to estimate the stability constant of the respective complex. The spectral changes of compound *I* under various concentrations of F^- ions are shown in Fig. 7a. The

Table 4. Hydrogen bond geometry for *I*

D—H···A	D—H	H···A	D···A	D—H···A
		Å		°
O1—H1A···N4	1.00(3)	1.77(3)	2.763(2)	172(3)
O2—H2A···N1^a	0.95(3)	1.78(3)	2.723(2)	171(3)
N5—H5B···N3^b	0.93(3)	2.66(3)	3.483(3)	148.4(19)
N5—H5C···O2^c	0.88(3)	2.33(3)	3.058(3)	140(2)

Symmetry codes: *a*) $-x + 1/2$, $y + 3/2$, $-z + 1/2$; *b*) $-x + 1$, $-y$, $-z + 1$; *c*) $-x + 1/2$, $y - 1/2$, $-z + 1/2$.

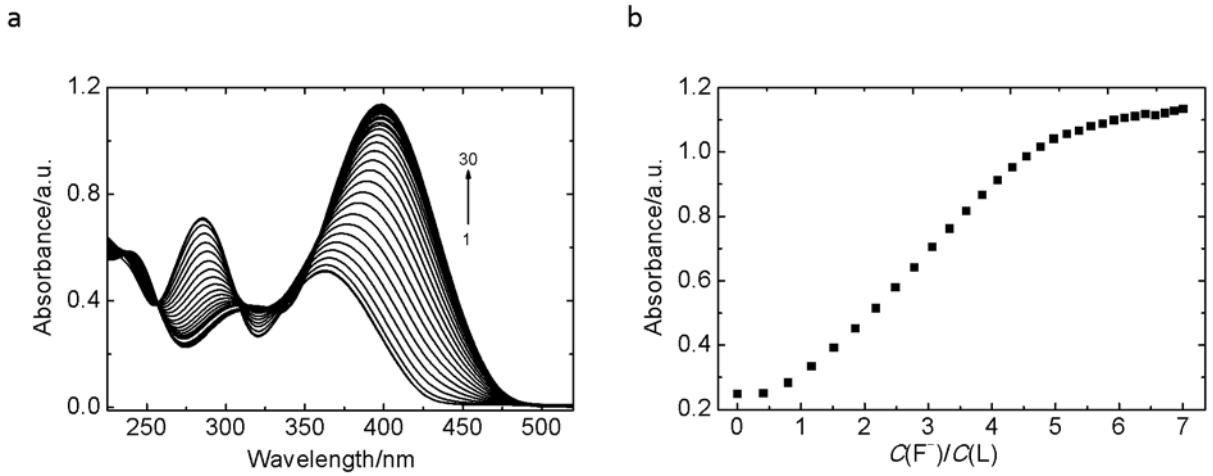

Fig. 7. Changes in absorption spectra upon titration of *I* ($c = 3 \times 10^{-5}$ mol L^{-1}) with TBAF (c = 0–2.10 $\times 10^{-4}$ mol L^{-1}) (lines 1–30) in CH_3CN (a). Titration plot to determine stability constant of complex between *I* and F^- at 400 nm (b).

addition of F^- ions caused a gradual decrease in the intensity of the peak at 285 nm and a batochromic shift from 362 nm to 400 nm ($\Delta\lambda = 38$ nm), followed by a change in colour of the solution from colourless to yellow. In the spectrum, there is only one isosbestic point at 257 nm. On the basis of the titration experiments, two types of equilibrium of strong complexes in CH_3CN were found (Fig. 7b). The stoichiometries of the complexes were 2 : 1 and 1 : 4 (I : F^-). It was not possible to calculate the binding constants of the fluoride complexes. Moreover, ligand I showed no UV-VIS absorption spectral changes and no colour in the presence of other anions in the sample of F^- ions (Fig. 8) as inspected by the naked eye. This is very important because many sensors for F^- ions suffer from interference from AcO^- and $H_2PO_4^-$ ions.

To investigate the anion-binding properties of ligand I in the presence of the anions studied and the role of the *para*-substituted hydroxyl group in the Schiff base, the ^{1}H NMR titration experiment in deuterated DMSO made it possible to distinguish the free sensor I and its complex with F^- ions. The spectra differed significantly, as shown in Fig. 9 and Table 5. Upon the addition of 2 eq. of TBAF, the signal at δ of 10.1 disappeared which may be due to the formation of an intramolecular hydrogen bond between the oxygen atom of the hydroxyl group and the F^- ions after

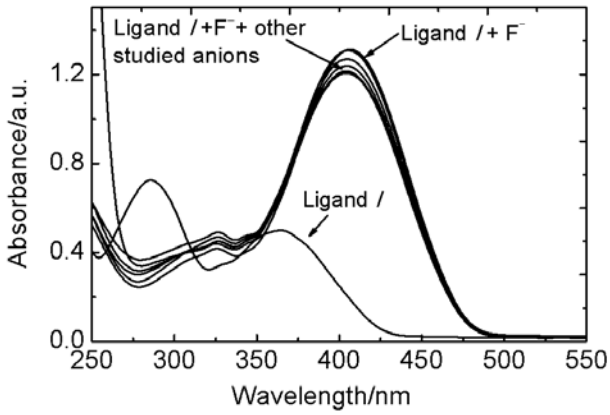

Fig. 8. UV-VIS spectra of sensor I ($c = 3 \times 10^{-5}$ mol L^{-1}) and changes to F^- ions (100 eq.) in the absence and presence of 100 eq. of various anions in CH_3CN.

deprotonation. In the case of the imine group in the absence of TBAF, the CH═N proton appeared as a singlet at δ of 8.52 (Fig. 9a), whereas in the presence of 2 eq. of F^- ions (Fig. 9b), the singlet was shifted up-field to δ of 8.07. There were significant changes in the ligand I spectrum in the aromatic part upon complexation were. All the aromatic hydrogen atoms of the pyridine units were shifted up-field. Analysis

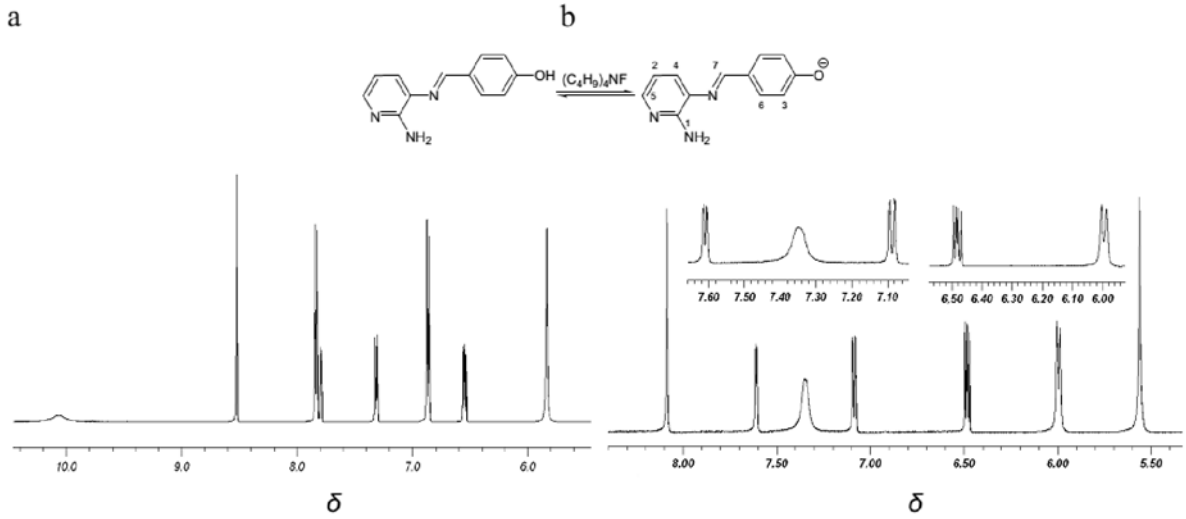

Fig. 9. ^{1}H NMR spectra of sensor I with addition of TBAF in DMSO-d_6 solution. I only (a); $I + F^-$ (2.0 eq.) (b).

Table 5. Chemical shift changes in ^{1}H NMR spectra (500 MHz) of sensor I in the presence of 2 eq. of TBAF in DMSO-d_6

Compound	1	2	3,3′	4	5	6,6′	7	8
				δ (Split)				
I	5.83 (s)	6.54 (dd)	6.86 (d)	7.31 (d)	7.79 (d)	7.82 (d)	8.52 (s)	10.1
$I + F^-$	5.55 (s)	6.47 (dd)	5.98 (d)	7.07 (d)	7.59 (d)	7.33 (s)	8.07 (s)	–
$\Delta\delta$	–0.28	–0.07	–0.88	–0.24	–0.20	–0.49	–0.45	–

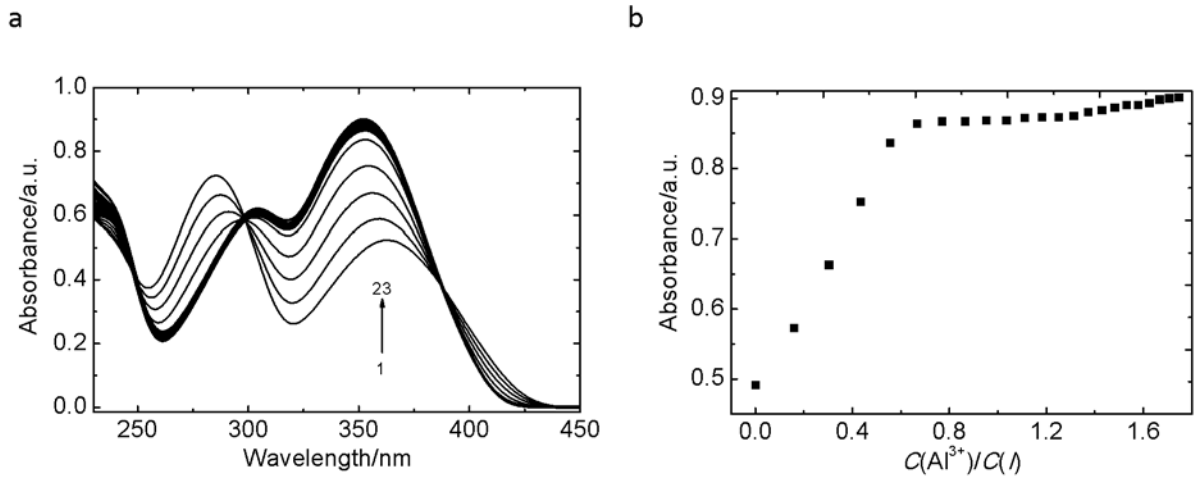

Fig. 10. Absorption spectra recorded in CH_3CN solution containing ligand I ($c = 3 \times 10^{-5}$ mol L^{-1}) and $Al(NO_3)_3$ (c = 0–5.24 × 10^{-5} mol L^{-1}) (lines 1–23) (a). Dependence of absorbance at 352 nm for ligand I with Al^{3+} ions (b).

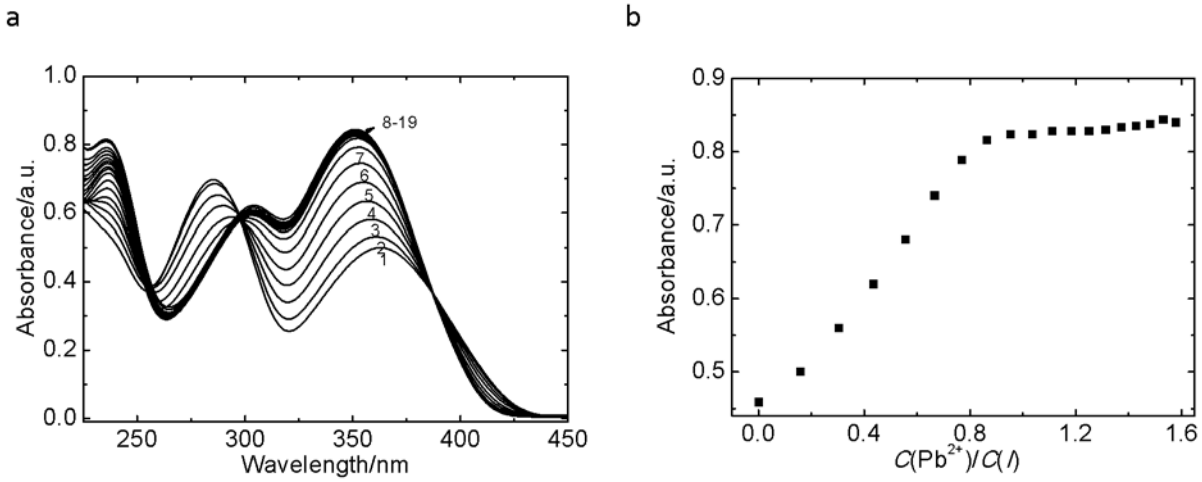

Fig. 11. UV-VIS spectral changes of ligand I ($c = 3 \times 10^{-5}$ mol L^{-1}) upon addition of $Pb(ClO_4)_2$ (c = 0–4.74 × 10^{-5} mol L^{-1}) (lines 1–19) (a). Dependence of absorbance at 350 nm for ligand I with Pb^{2+} ions (b).

of the chemical shift changes for the aromatic proton signals confirmed the phenolate form, which can be seen in the up-field shift of 3,3' ($\Delta\delta$ = –0.88) and 6,6' ($\Delta\delta$ = –0.49) protons. Simultaneously, two protons 6,6' (doublet) at δ of 7.82 were coupled to each other and formed a single peak at δ of 7.33. In the presence of 3 eq. of TBAF a new triplet at δ of 16.1 with J = 124 Hz appeared, which was due to the deprotonation of the chromogenic sensor and may be attributed to the HF_2^- dimer. Changes in the chemical shift values of the aromatic protons, the amino group and the disappearance of the —OH singlet upon 2 eq. of TBAF indicated a strong H-bond interaction between the sensor-recognition site and the F^- ions resulting in the appearance of the yellow colour.

In addition, ligands *I–II* were treated with transition metal ions and heavy metal ions to evaluate the optical response in CH_3CN. The most notable changes in the absorption were found in the presence of Al^{3+}, Pb^{2+}, Zn^{2+} and Cu^{2+} ions (Figs. 10–16). The addition of metal ions such as Ni^{2+}, Co^{2+} and Fe^{2+} to the solution of ligands in CH_3CN did not exhibit any notable spectral change; the absorption spectra of the ligands only increased the intensity of the main band. Figs. 10–12 show that the additions of Al^{3+}, Pb^{2+}, Cu^{2+} ions to I induced similar spectral changes. Ligand I had absorption peaks at about 285 nm and 362 nm in the absence of cations. With the increase in cations' concentration, the band intensity at 285 nm decreased and the intensity of the absorbance at about 350 nm increased. The formation of two clear isosbestic points at 298 nm and 388 nm (for Al^{3+} and Pb^{2+} ions) and one at 374 nm for Cu^{2+} indicates the formation of a stable complex with a certain stoichiometric ratio between the ligands and cations examined (Table 6). Although ligand I exhibited similar spectral changes for selected cations at the same wavelength, the intensity of the spectral response was different

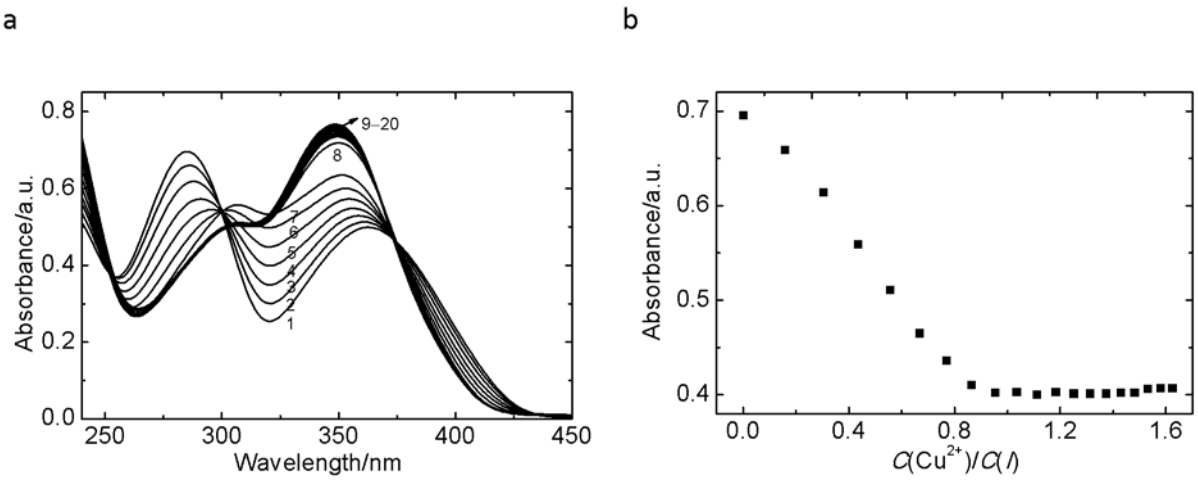

Fig. 12. Changes in UV-VIS absorption spectrum of ligand I ($c = 3 \times 10^{-5}$ mol L^{-1}) with $Cu(ClO_4)_2$ (c = 0–4.87×10^{-5} mol L^{-1}) (lines 1–20) in CH_3CN solution (a). Titration plot to determine stability constant of complex between $I$and Cu^{2+} (1 : 1) at 285 nm (b).

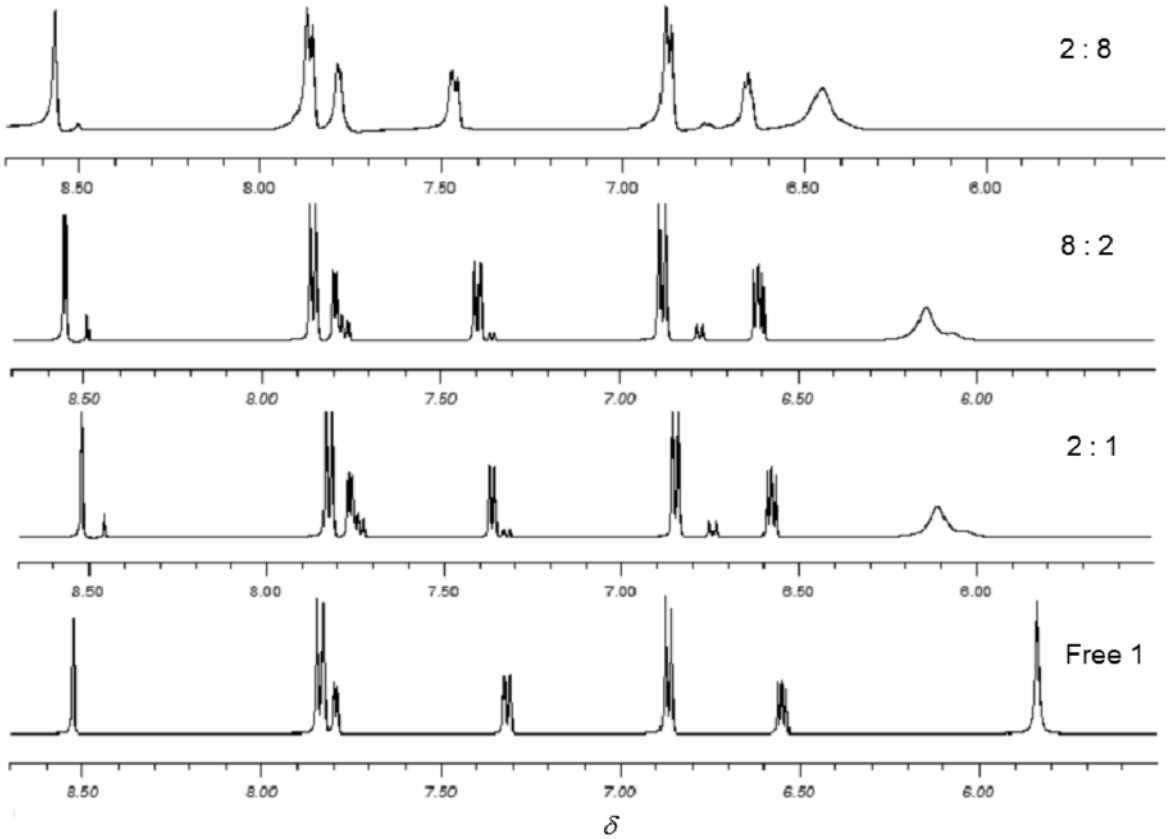

Fig. 13. ^1H NMR spectra of free I and its complex with $Al(NO_3)_3$ dissolved in DMSO-d_6 (I : Al^{3+}).

upon the addition of an equivalent amount of Al^{3+}, Pb^{2+} and Cu^{2+}. The stoichiometries of the complexes were 1 : 1 (Pb^{2+}, Zn^{2+}, Cu^{2+}) and 1 : 2 for (Al^{3+} ions).

The mechanism of the cation-binding properties of I with Al^{3+} ions was investigated by the ^1H NMR titration experiment in DMSO-d_6 (Fig. 13). ^1H NMR spectral analysis showed that the signals corresponding to the protons of the hydroxyl and imine groups were shifted slightly downfield which suggests the formation of a complex in protonated form. In the case of the solution containing I and Al^{3+} ions in a molar ratio of 1 : 4, the addition of $Al(NO_3)_3$ caused a gradual broadening of the complex signals. The N—H protons of I δ of around 5.83 displayed a downfield shift to δ of 6.44. The formation of new small

Table 6. Overall stability constants of Cu^{2+}, Pb^{2+}, Al^{3+} and Zn^{2+} complexes with ligands *I–II*

Compound	$Cu^{2+,a}$	$Pb^{2+,a}$	Al^{3+}	$Zn^{2+,a}$
I	$(3.90 \pm 0.37) \times 10^3$	$(7.80 \pm 0.12) \times 10^3$	$(8.40 \pm 0.15) \times 10^5$	$(1.20 \pm 0.46) \times 10^4$
Complex stoichiometry	1 : 1	1 : 1	1 : 2	1 : 1
II	$(5.70 \pm 0.05) \times 10^3$	$(5.30 \pm 0.20) \times 10^3$	$(3.50 \pm 0.41) \times 10^5$	$(1.80 \pm 0.42) \times 10^4$
Complex stoichiometry	1 : 1	1 : 1	1 : 2	1 : 1

a) Determined using Benesi–Hildebrand relation.

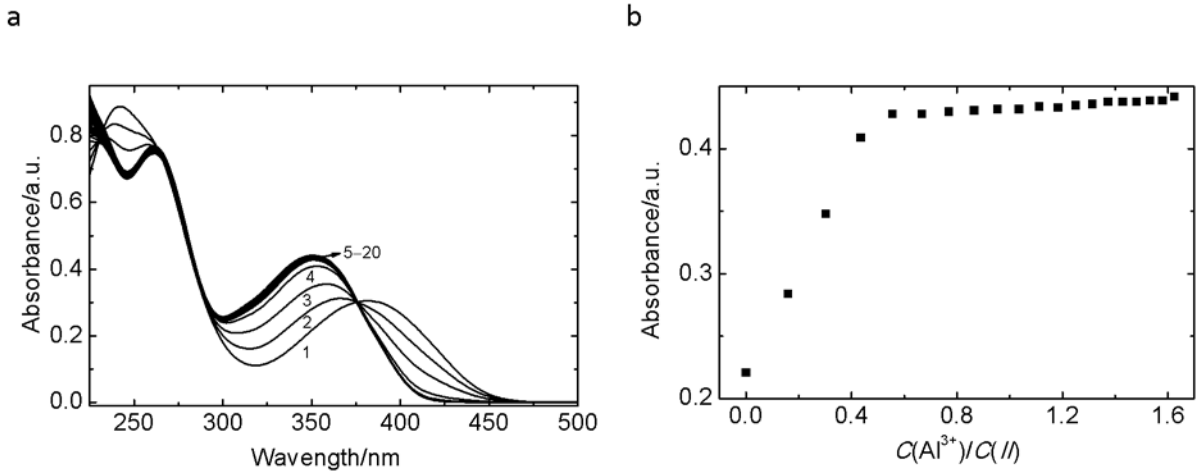

Fig. 14. UV-VIS titration of compound *II* ($c = 3 \times 10^{-5}$ mol L^{-1}) with $Al(NO_3)_3$ ($c = 0$–4.87×10^{-5} mol L^{-1}) (lines 1–20) (a). Dependence of absorbance at 351 nm for ligand *II* with Al^{3+} ions (b).

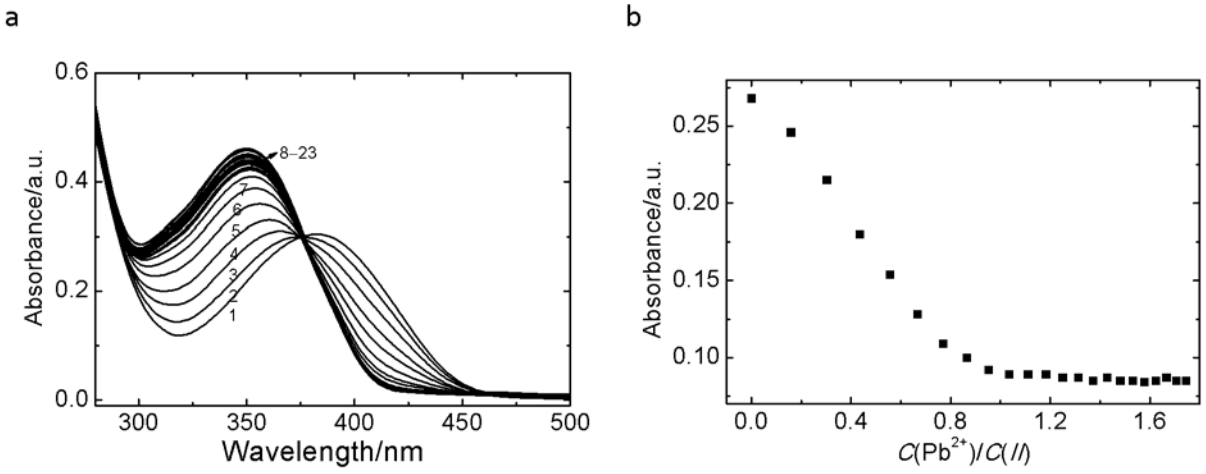

Fig. 15. Absorption spectra recorded for CH_3CN solution containing ligand *II* ($c = 3 \times 10^{-5}$ mol L^{-1}) and $Pb(ClO_4)_2$ ($c = 0$–5.24×10^{-5} mol L^{-1}) (lines 1–23) (a). Dependence of absorbance at 350 nm for ligand *II* with Pb^{2+} ions (b).

signals occurred when a 2 : 1 (*I* : $Al(NO_3)_3$) ratio was achieved. A gradual addition of salt caused the largest changes especially in the pyridine region and a slightly smaller contribution of CH═N protons. These spectral changes suggest that the free exchange of Al^{3+} ions promotes the formation of two complexes during the titration experiments in solution, hence. It was difficult to assess the structure of the resulting complexes. The spectral changes observed could imply that ionisation of the amino groups was achieved throughout the complexation process.

Figs. 14–16 show the impact of various cations on the UV spectrum of ligand *II* in a CH_3CN solution. Compound *II* had certain absorption peaks at 242 nm and 381 nm. Upon the successive addition of cations (Al^{3+}, Pb^{2+}, Cu^{2+}) to ligand *II*, the intensity of absorbance at 242 nm decreased, while the intensity of the peak at 381 nm was shifted to a shorter wavelength. In the case of Al^{3+} ions, a new maximum absorption was found at 350 nm with one clear

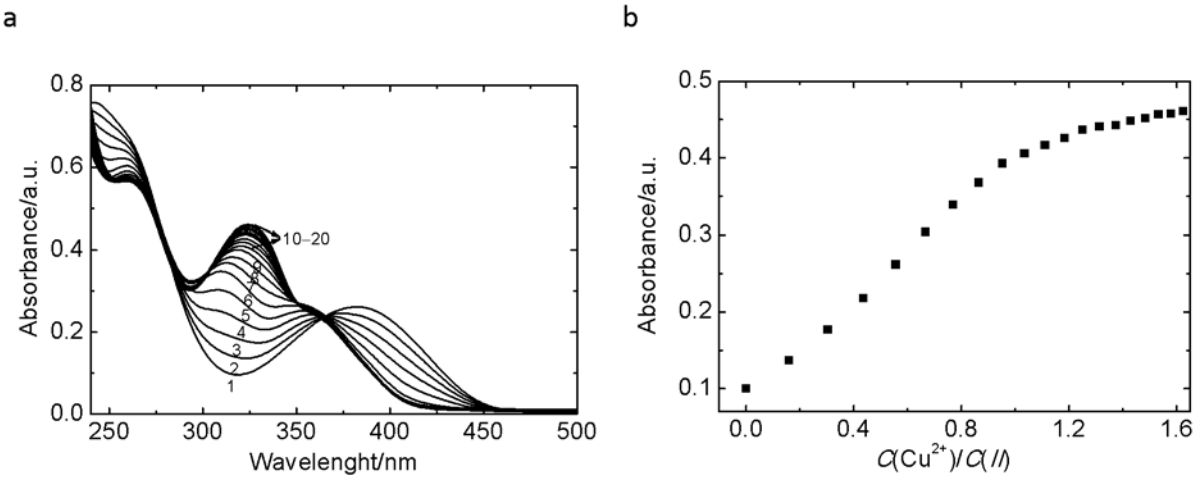

Fig. 16. Changes in UV-VIS absorption spectrum of ligand *II* ($c = 3 \times 10^{-5}$ mol L^{-1}) with $Cu(ClO_4)_2$ (c = 0–4.87 $\times$ 10^{-5} mol L^{-1}) (lines 1–20) in CH_3CN solution (a). Titration plot to determine stability constant of complex between *II* and Cu^{2+} (1 : 1) at 324 nm (b).

isosbestic point at 376 nm (Fig. 14). A molar ratio plot revealed that, under the titration experiments, a complex of 1 : 2 (Al^{3+} : *II*) was established. Furthermore, the absorption spectra of *II* with Pb^{2+} and Cu^{2+} with various concentrations of ions exhibited a hypsochromic shift; the absorption band at 381 nm was shifted to 350 nm and 324 nm, respectively. As the concentration of cations increased, one isosbestic point at 376 nm for Pb^{2+} and 364 nm Cu^{2+} complex was formed. The binding constants for the 1 : 1 complexes were obtained from the Benesi–Hildebrand equation (Table 6).

The binding ability (b) of ligands *I* and *II* with the examined cations is in the order of $b(Al^{3+}) > b(Zn^{2+}) > b(Pb^{2+}) > b(Cu^{2+})$; $b(Al^{3+}) > b(Zn^{2+}) > b(Cu^{2+}) \geq b(Pb^{2+})$, respectively. Compounds *I* and *II* exhibit the highest binding ability with Al^{3+} ions. The similar patterns of spectroscopic changes in the absorption spectra may suggest that the substituent in the phenyl ring does not participate in the complexation process. Moreover, it was presumed that cations are incorporated between the imino and amino groups. However, the different patterns of spectroscopic changes in the absorption spectra between the F^- ions and the previously reported studies may confirm the hydroxyl group to be essential in the complexation properties towards anions.

The metal Schiff base complexes derived from salicylaldehyde and diaminopyridine have been widely studied. The Schiff base ligands behave like O, N donor bidentate for copper, nickel, iron, cobalt, zinc and ruthenium ions. Asymmetrical Schiff bases with Cu, Ni and Fe(III) complexes have also been prepared. In the event that the free amino group is still present, coordination also occurs through the amino and CH═N groups. However, the coordination chemistry and behaviour of these compounds as sensors using UV-VIS spectroscopy have not yet received any attention in the literature.

Table 7. Calculated parameters for complex of *I*

Compound *I*	Cu^{2+} : *I*	Pb^{2+} : *I*	Zn^{2+} : *I*
N1····X	5.565	5.833	5.247
N2····X	3.447	4.045	3.143
N3····X	3.512	3.781	3.121
C6····X	4.228	4.343	3.886
O1····X	6.406	6.430	6.369

Molecular simulation

Computational simulations of the Schiff base ligand and the metal complexes were carried out using Gaussian 03 software with the B3LYP and 6-31++G(dp) basis set at the density functional theory (DFT) level. The optimised calculated geometry in Fig. 17 reveals molecule *I* not to be in the same plane. The binding affinity of this ligand was determined toward several cations and F^- ions. The introduction of cations (Cu^{2+}, Pb^{2+}, Zn^{2+}) into ligand *I* shows that, in all cases, cations were located in the cavity formed between the imino bonds and the amino groups. The absence of changes in the hydroxyl group suggests that it is not engaged in the complex, thereby confirming the earlier hypothesis. Table 7 presents the important parameters of the experimental data between *I* and the metal cations studied. The calculated distances between the imino bonds and the cations are the shortest for Zn^{2+} ions. The bond lengths in the case of different complexes increase with the bigger and different geometrical shape of the guest. The optimised global minima of the Schiff base ligand *I*

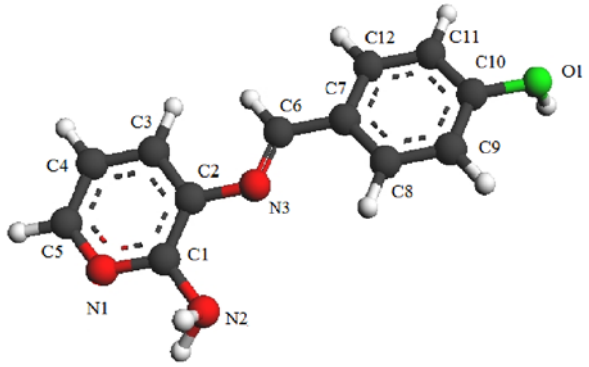

Fig. 17. DFT optimised structure of compound *I*.

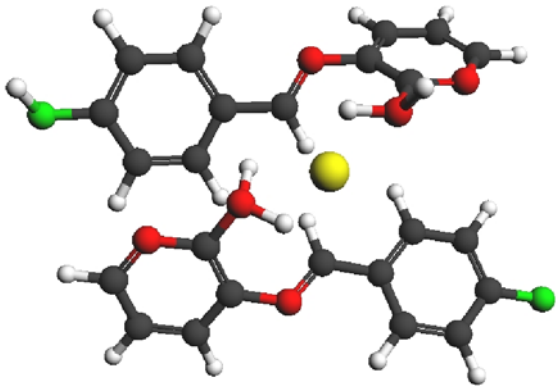

Fig. 19. Optimised geometry of Al^{3+} : *I* complex.

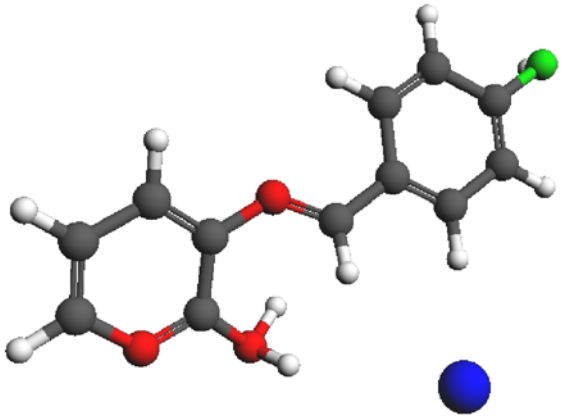

Fig. 18. Optimised structure of Cu^{2+} : *I* complex.

and Cu^{2+}, Al^{3+} complexes are presented in Figs. 18–19. In addition, the introduction of F^- ions into ligand *I* led to a reorganisation of the structure to a more rigid system. Clearly, the O—H moieties in the structure *I* are involved in the complexation of F^- ions by relatively strong hydrogen interactions. The distance between the intramolecular hydrogen bonds (O—H···F) is 2.109 Å. Fluorine ion is the smallest ion and can fit between two molecules and form a 2 : 1 stable complex.

Conclusions

The spectroscopic properties of Schiff bases' behaviour depend on the nature and position of the substituent attached to the molecule. Induction of the electron-withdrawing group such as NO_2 into the sensor facilities the creation of a possible sensitive and complexing molecule. In order to increase the selectivity of the ligand, the free hydroxyl group was introduced the *para* position on the aromatic ring. Accordingly, a new mono Schiff base derived from 2,3-diaminopyridine *I–II* was synthesised. The spectroscopic properties were investigated by UV-VIS and ^1H NMR spectroscopic methods and by the DFT method. UV-VIS measurements showed that ligand *I* selectively recognised F^- ions. A naked-eye colour change was not observed upon the addition of other anions. Furthermore, the synthesised ligands were used as sensing materials for transition metal cations and heavy metal cations. The addition of Al^{3+}, Zn^{2+}, Pb^{2+} and Cu^{2+} ions caused a gain and hypsochromic shift effect of the maximum absorption band of the compounds presented. The values of the binding constant are highest for Al^{3+} complexes. The presence of the amino and hydroxyl groups strongly influences the complexing ability of molecules.

Acknowledgements. The financial support for this work received from Gdansk University of Technology, grant no. BW 020331/006 DS 020223/003 is gratefully acknowledged. The authors wish to thank Professor J. Biernat for the invaluable assistance in the implementation of research and preparation of the manuscript.

Supplementary data

Complete crystallographic data for the structure reported in this paper were deposited with the Cambridge Crystallographic Data Centre as Supplementary Publication No CCDC 988906. Copies of the data can be obtained free of charge from the CCDC, 12 Union Road, Cambridge CB2 1EZ, UK (tel.: +44-1223-336-408; fax: +44-1223-336-033, e-mail: deposit@ccdc.cam.ac.uk).

References

Abdel-Rahman, L. H., El-Khatib, R. M., Nassr, L. A. E., Abu-Dief, A. M., & El-Din Lashin, F. (2013). Design, characterization, teratogenicity testing, antibacterial, antifungal and DNA interaction of few high spin Fe(II) Schiff base amino acid complexes. *Spectrochimica Acta Part A*, *111*, 266–276. DOI: 10.1016/j.saa.2013.03.061.

Afkhami, A., Bagheri, H., Khoshsafar, H., Saber-Tehrani, M., Tabatabaee, M., & Shirzadmehr, A. (2012). Simultaneous trace-levels determination of Hg(II) and Pb(II) ions in various samples using a modified carbon paste electrode based on multi-walled carbon nanotubes and a new synthesized

Schiff base. *Analytica Chimica Acta*, *746*, 98–106. DOI: 10.1016/j.aca.2012.08.024.

Amin, R. M., Abdel-Kader, N. S., & El-Ansary, A. L. (2012). Microplate assay for screening the antibacterial activity of Schiff bases derived from substituted benzopyran-4-one. *Spectrochimica Acta Part A*, *95*, 517–525. DOI: 10.1016/j.saa.2012.04.042.

Azadbakht, R., Almasi, T., Keypour, H., & Rezaeivala, H. (2013). A new asymmetric Schiff base system as fluorescent chemosensor for Al^{3+} ion. *Inorganic Chemistry Communications*, *33*, 63–67. DOI: 10.1016/j.inoche.2013.03.014.

Aziz, A. A. A. (2013). A novel highly sensitive and selective optical sensor based on a symmetric tetradentate Schiff-base embedded in PVC polymeric film for determination of Zn^{2+} ion in real samples. *Journal of Luminescence*, *143*, 663–669. DOI: 10.1016/j.jlumin.2013.06.020.

Carreño, A., Gacitua, M., Schott, E., Zarate, X., Manriquez, J. M., Preite, M., Ladeira S., Castel, A., Pizarro, N., Vega, A., Chavez, I., & Arratia-Perez, R. (2015). Experimental and theoretical studies of the ancillary ligand (*E*)-2-((3-amino-pyridin-4-ylimino)-methyl)-4,6-di-tert-butylphenol in the rhenium(I) core. *New Journal of Chemistry*, *39*, 5725–5734. DOI: 10.1039/c5nj00772k.

Cimerman, Z., Galešić, N., & Bosner, B. (1992). Structure and spectroscopic characteristics of Schiff bases of salicylaldehyde with 2,3-diaminopyridine. *Journal of Molecular Structure*, *274*, 131–144. DOI: 10.1016/0022-2860(92)80152-8.

Cimerman, Z., Galic, N., & Bosner, B. (1997). The Schiff bases of salicylaldehyde and aminopyridines as highly sensitive analytical reagents. *Analytica Chimica Acta*, *343*, 145–153. DOI: 10.1016/s0003-2670(96)00587-9.

Dai, C. H., & Mao, F. L. (2013). Structure of a new Schiff base cobalt(III) complex with antibacterial activity. *Journal of Structural Chemistry*, *54*, 624–629. DOI: 10.1134/s0022476613030244.

Devaraj, S., Tsui, Y. K., Chiang, C. Y., & Yen, Y. P. (2012). A new dual functional sensor: Highly selective colorimetric chemosensor for Fe^{3+} and fluorescent sensor for Mg^{2+}. *Spectrochimica Acta Part A*, *96*, 594–599. DOI: 10.1016/j.saa.2012.07.032.

Dubey, P. K., & Ratnam, C. V. (1977). Formation of heterocyclic rings containing nitrogen: Part XXVI – Condensation of pyridine 2,3-diamine with aromatic aldehydes. *Proceedings of the Indian Academy of Sciences – Section A*, *85*, 204–209. DOI: 10.1007/bf03049482.

Erdemir, S., Kocyigit, O., Alici, O., & Malkondu, S. (2013). 'Naked-eye' detection of F^- ions by two novel colorimetric receptors. *Tetrahedron Letters*, *54*, 613–617. DOI: 10.1016/j.tetlet.2012.11.138.

Frisch, M. J., Trucks, G. W., Schlegel, H. B., Scuseria, G. E., Robb, M. A., Cheeseman, J. R., Montgomery, J. A., Jr., Vrenen, T., Kudin, K. N., Burant, J. C., Illa, J. M., Iyengar, S. S., Tomasi, J., Barone, V., Mennuci, B., Cossi, M., Scalmani, G. Rega, N., Petersson, G. A., Nakatsuji, H., Hada, M., Ehara, M., Toyota, K., Fukuda, K. R., Hasegawa, J., Ishida, M., Nakajima, T., Honda, Y., Kitao, O., Nakai, H., Klene, M., Li, X., Knox, J. E., Hratchian, H. P., Cross, J. B., Bakken, V., Adamo, V. C., Jaramillo, J., Gomperts, R., Stratmann, R. E., Yazyev, O., Ausin, A. J., Cammi, R., Pomelli, C., Ochterski, J., Ayala, P. Y., Morokuma, K., Voth, G. A., Salavador, P., Dannenberg, J. J., Zakrzewski, V. G., Dopprich, S., Daniels, A. D., Strain. M. C., Farkas, O., Malick, D. K., Rabuck, A. D., Raghavashari, K., Foresman, J. B., Orlitz, J. V., Cui, Q., Baboul, A., Cliffors, S., Cioslowski, J., Stefanov, B. B., Liu, G., Liashenko, A., Piskorz, P., Komaromo, I., Martin, R. L., Fox, D. J., Keith, T., Al-Laham, M. A., Peng, C. Y., Nanyakkara, A., Challacombe, M., Gill, P. M. W., Johnson, B., Chen, W., Wong, J. L. Gonzalez, C., & Pople, J. (2004). Gaussian 03, Revision 03 [computer software]. Wallingford, CT, USA: Gaussian Inc.

Grivani, G., & Akherati, A. (2013). Polymer-supported bis (2-hydroxyanyl) acetylacetonato molybdenyl Schiff base catalyst as effective, selective and highly reusable catalyst in epoxidation of alkenes. *Inorganic Chemistry Communications*, *28*, 90–93. DOI: 10.1016/j.inoche.2012.11.015.

Gupta, V. K., Singh, A. K., Ganjali, M. R., Norouzi, P., Faridbod, F., & Mergu, N. (2013). Comparative study of colorimetric sensors based on newly synthesized Schiff bases. *Sensors and Actuators B*, *182*, 642–651. DOI: 10.1016/j.snb.2013.03.062.

Heo, Y., Kang, Y. Y., Palani, T., Lee, J., & Lee, S. (2012). Synthesis, characterization of palladium hydroxysalen complex and its application in the coupling reaction of arylboronic acids: Mizoroki–Heck type reaction and decarboxylative couplings. *Inorganic Chemistry Communications*, *23*, 1–5. DOI: 10.1016/j.inoche.2012.05.013.

Huang, C. Y., Wan, C. F., Chir, J. L., & Wu, A. T. (2013). A Schiff-based colorimetric fluorescent sensor with potential for detection of fluoride ions. *Journal of Fluorescence*, *23*, 1107–1111. DOI: 10.1007/s10895-013-1257-z.

Jarvo, E. R., Lawrence, B. M., & Jacobsen, E. N. (2005). Highly enantio- and regioselective quinone Diels–Alder reactions catalyzed by a tridentate [(Schiff base)CrIII] complex. *Angewandte Chemie International Edition*, *44*, 6043–6046. DOI: 10.1002/anie.200502176.

Jeong, T., Lee, H. K., Jeong, D. C., & Jeon, S. (2005). A lead(II)-selective PVC membrane based on a Schiff base complex of *N*,*N*′-bis(salicylidene)-2,6-pyridinediamine. *Talanta*, *65*, 543–548. DOI: 10.1016/j.talanta.2004.07.016.

Jeewoth, T., Bhowon, M. G., & Wah, H. L. K. (1999). Synthesis, characterization and antibacterial properties of Schiff bases and Schiff base metal complexes derived from 2,3-diamino-pyridine. *Transition Metal Chemistry*, *24*, 445–448. DOI: 10.1023/a:1006917704209.

Ji, C., Day, S. E., & Silvers, W. C. (2008). Catalytic reduction of 1- and 2-bromooctanes by a dinickel(I) Schiff base complex containing two salen units electrogenerated at carbon cathodes in dimethylformamide. *Journal of Electroanalytical Chemistry*, *622*, 15–21. DOI: 10.1016/j.jelechem.2008.04.023.

Jiménez-Sánchez, A., Farfán, N., & Santillan, R. (2013). A reversible fluorescent–colorimetric Schiff base sensor for Hg^{2+} ion. *Tetrahedron Letters*, *54*, 5279–5283. DOI: 10.1016/j.tetlet.2013.07.072.

Kleij, A. W., Tooke, D. M., Spek, A. L., & Reek, J. N. H. (2005). A convenient synthetic route for the preparation of nonsymmetric metallo–salphen complexes. *European Journal of Inorganic Chemistry*, *22*, 4626–4632. DOI: 10.1002/ejic.200500628.

Kumar, K. S., Ganguly, S., Veerasamy, R., & De Clercq, E. (2010). Synthesis, antiviral activity and cytotoxicity evaluation of Schiff bases of some 2-phenyl quinazoline-4(3)*H*-ones. *European Journal of Medicinal Chemistry*, *45*, 5474–5479. DOI: 10.1016/j.ejmech.2010.07.058.

Kumar, M. S., Kumar, S. L. A., & Sreekanth, A. (2013). An efficient triazole-based fluorescent "turn-on" receptor for naked-eye recognition of F^- and AcO^-: UV-visible, fluorescence and ^1H NMR studies. *Materials Science and Engineering: C*, *33*, 3346–3352. DOI: 10.1016/j.msec.2013.04.018.

Lin, C. Y., Huang, K. F., & Yen, Y. P. (2013). A new selective colorimetric and fluorescent chemodosimeter for HSO_4^- based on hydrolysis of Schiff base. *Spectrochimica Acta Part A*, *115*, 552–558. DOI: 10.1016/j.saa.2013.06.083.

Liu, G., & Shao, J. (2013). Ratiometric fluorescence and colorimetric sensing of anion utilizing simple Schiff base derivatives. *Journal of Inclusion Phenomena and Macrocyclic Chemistry*, *76*, 99–105. DOI: 10.1007/s10847-012-0177-x.

Ourari, A., Khelafi, M., Aggoun, D., Jutand, A., & Amatore, C. (2012). Electrocatalytic oxidation of organic substrates with molecular oxygen using tetradentate ruthenium(III)–Schiff base complexes as catalysts. *Electrochimica Acta*, *75*, 366–370. DOI: 10.1016/j.electacta.2012.05.021.

Qiao, X., Ma, Z. Y., Xie, C. Z., Xue, F., Zhang, Y. W., Xu, J. Y., Qiang, Z. Y., Lou, J. S., Chen, G. J., & Yan, S. P. (2011). Study on potential antitumor mechanism of a novel Schiff base copper(II) complex: Synthesis, crystal structure, DNA binding, cytotoxicity and apoptosis induction activity. *Journal of Inorganic Biochemistry*, *105*, 728–737. DOI: 10.1016/j.jinorgbio.2011.01.004.

Reena, V., Suganya, S., & Velmathi, S. (2013). Synthesis and anion binding studies of azo-Schiff bases: Selective colorimetric fluoride and acetate ion sensors. *Journal of Fluorine Chemistry*, *153*, 89–95. DOI: 10.1016/j.jfluchem.2013.05.010.

Şahin, Z. M., Doğancı, E., Yıldız, S. Z., Tuna, M., Yılmaz, F., Yerli, Y., & Görür, M. (2010). Synthesis and characterization of two-armed poly(ε-caprolactone) polymers initiated by Schiff's base complexes of copper(II) and nickel(II). *Synthetic Metals*, *160*, 1973–1980. DOI: 10.1016/j.synthmet.2010.07.018.

Schiff, H. (1866). Eine neue Reihe organischer Diamine. *Annalen der Chemie und Pharmacie*, *140*, 92–137. DOI: 10.1002/jlac.18661400106. (in German)

Schilf, W., Kamieński, B., Rozwadowski, Z., Ambroziak, K., Bieg, B., & Dziembowska, T. (2004). Solid state ^{15}N and ^{13}C NMR study of dioxomolybdenum(VI) complexes of Schiff bases derived from *trans*-1,2-cyclohexanediamine. *Journal of Molecular Structure*, *700*, 61–65. DOI: 10.1016/j.molstruc.2003.11.055.

Sen, S., Mukherjee, M., Chakrabarty, K., Hauli, I., Mukhopadhyay, S. K., & Chattopadhyay, P. (2013). Cell permeable fluorescent receptor for detection of $H_2PO_4^-$ in aqueous solvent. *Organic & Biomolecular Chemistry*, *11*, 1537–1544. DOI: 10.1039/c2ob27201f.

Sheldrick, G. M. (2008). A short history of SHELX. *Acta Crystallographica Section A*, *64*, 112–122. DOI: 10.1107/s0108767307043930.

Udhayakumari, D., Saravanamoorthy, S., & Velmathi, S. (2012). Colorimetric and fluorescent sensing of transition metal ions in aqueous medium by salicylaldimine based chemosensor. *Materials Science and Engineering: C*, *32*, 1878–1882. DOI: 10.1016/j.msec.2012.05.005.

Waldeck, D. H. (1991). Photoisomerization dynamics of stilbenes. *Chemical Reviews*, *91*, 415–436. DOI: 10.1021/cr00003a007.

Yang, Y. X., Xue, H. M., Chen, L. C., Sheng, R. L., Li, X. Q., & Li, K. (2013). Colorimetric and highly selective fluorescence "turn-on" detection of Cr^{3+} by using a simple Schiff base sensor. *Chinese Journal of Chemistry*, *31*, 377–380. DOI: 10.1002/cjoc.201200852.

Yao, L. H., Wang, L., Zhang, J. F., Tang, N., & Wu, J. C. (2012). Ring opening polymerization of L-lactide by an electron-rich Schiff base zinc complex: An activity and kinetic study. *Journal of Molecular Catalysis A*, *352*, 57–62. DOI: 10.1016/j.molcata.2011.10.012.

Yıldız, M., Ünver, H., Erdener, D., Kiraz, A., & İskeleli, N. O. (2009). Synthesis, spectroscopic studies and crystal structure of (*E*)-2-(2,4-dihydroxybenzylidene)thiosemicarbazone and (*E*)-2-[(1*H*-indol-3-yl)methylene]thiosemicarbazone. *Journal of Molecular Structure*, *919*, 227–234. DOI: 10.1016/j.molstruc.2008.09.008.

Yuan, X. J., Wang, R. Y., Mao, C. B., Wu, L., Chu, C. Q., Yao, R., Gao, Z. Y., Wu, B. L., & Zhang, H. Y. (2012). New Pb(II)-selective membrane electrode based on a new Schiff base complex. *Inorganic Chemistry Communications*, *15*, 29–32. DOI: 10.1016/j.inoche.2011.09.031.

Zhang, L., Ni, X. F., Sun, W. L., & Shen, Z. Q. (2008). Polymerization of isoprene catalyzed by neodymium heterocyclic Schiff base complex. *Chinese Chemical Letters*, *19*, 734–738. DOI: 10.1016/j.cclet.2008.03.007.

Zhou, G. P., Hui, Y. H., Wan, N. N., Liu, Q. J., Xie, Z. F., & Wang, J. D. (2012a). $Mn(OAc)_2$/Schiff base as a new efficient catalyst system for the Henry reaction of nitroalkanes with aldehydes. *Chinese Chemical Letters*, *23*, 690–694. DOI: 10.1016/j.cclet.2012.04.018.

Zhou, Y. M., Zhou, H., Zhang, J. L., Zhang, L., & Niu, J. Y. (2012b). Fe^{3+}-selective fluorescent probe based on aminoantipyrine in aqueous solution. *Spectrochimica Acta Part A*, *98*, 14–17. DOI: 10.1016/j.saa.2012.08.025.